Study of Critical Phenomena of Polystyrene–Poly(vinyl Methyl Ether) Blends by Solid State NMR

C. W. CHU, L. C. DICKINSON, and JAMES C. W. CHIEN,* *Department of Polymer Science and Engineering, University of Massachusetts, Amherst, Massachusetts 01003*

Synopsis

Thermally induced phase separation in PS/PVME blends was studied by solid state NMR. The proton spin–lattice relaxation in both the laboratory and the rotating frame were measured for the entire range of blend composition. Under conditions in which the blends are said to be compatible by other techniques $T_{1\rho}^{H}$ results obtained at −5°C showed microheterogeneity at a 10-Å scale. $T_{1\rho}^{H}$ values at room temperature are closer to the longer relaxation time of PS than that expected from simple weighted average of the relaxation times of the constituent homopolymers. This indicates incomplete averaging by spin diffusion and a restraining effect of PS on segmental motions of PVME. The blends were heated to cause phase separation and quenched. From the biphasic decay of ^{13}C magnetization, the compositions of the separated phases were estimated to give a lower critical solution temperature phase diagram. NMR relaxation in PVME blends with PS molecular weights of 9, 100, and 900 K were compared.

INTRODUCTION

Lower critical solution temperature (LCST) phase separation behavior is generally expected for polymer–polymer systems.[1-3] Polystyrene/poly(vinyl methyl ether) (PS/PVME) was the first polymer pair for which thermally induced phase separation was observed.[4] Samples cast from chlorinated solvents are phase separated; blend samples freeze-dried or cast from aromatic solvents are said to be compatible. Dielectric relaxation, however, suggests that toluene cast blends may not be so intimately mixed as in a copolymer.[5] As monitored by excimer fluorescence from PS,[6] the phase separation initially shows a linear concentration change with time in accordance with the simple theory for spinodal decomposition,[7] followed by slower processes. Conventional light scattering has been used[8] to obtain the spinodal curve and diffusion constants; resolved light scattering was employed to study nucleation and growth.[9] The temperature and composition dependence of the interaction parameter has been determined by neutron scattering,[10] the technique also revealed differences in phase separation kinetics for d^8-PS and h^8-PS/PVME blends.[11] An FTIR study showed small changes in the out-of-plane CH bending and C—OCH_3 vibration of PVME suggesting that these molecular regions are involved in some specific interaction with PS in the blend.[12] Kwei and co-workers[13-15] investigated the PS/PVME blend thoroughly with dilatometry, solvent vapor diffusion rates,

* To whom correspondence should be addressed.

Journal of Applied Polymer Science, Vol. 41, 2311–2325 (1990)
© 1990 John Wiley & Sons, Inc. CCC 0021-8995/90/9-102311-15$04.00

cloud point, optical microscopy, and broad-line ^{1}H-NMR. The spinodal decomposition was found to occur with negative diffusion constant and negative interaction parameter as expected.

In the pioneering ^{1}H-NMR study,[13] 50 PS/50 PVME blend samples were held for 30 min or more at 130°C yielding T_1 and T_2 data, which indicate the material to be microheterogeneous. The PVME and PS chains are incompletely mixed on the segmental scale. Subsequent two-dimensional ^{1}H-NMR work showed[16a] qualitatively some mixing within magnetic dipolar interaction distances. Blends prepared by precipitation with petroleum ether from toluene solution were found to contain both pure and mixed domains of PS by selective proton spin diffusion NMR.[16b] The degree of intermolecular mixing had also been investigated with ^{13}C-NMR,[17] including the Goldman–Shen spin diffusion technique[18] and on blends of d^8-PS/PVME.[19]

This work was undertaken to exploit the cross-polarization magic-angle spinning (CP-MAS) ^{13}C-NMR technique in determining an LCST phase diagram. Though there have been prior NMR studies cited above, the present work covers a much wider blend composition range and the $T_{1\rho}^{H}$ measurements probe domains approximately an order of magnitude smaller than earlier T_1^H measurements.

EXPERIMENTAL

Polystyrene ($M_n = 9 \times 10^3$, $M_w/M_n = 1.06$, $M_n = 10^5$, $M_w/M_n = 1.06$, $M_n = 9 \times 10^8$, $M_w/M_n = 1.1$) were from Pressure Chemicals. Poly(vinylmethyl ether), purchased from Aldrich as a 50% solution in toluene, was either dried in a vacuum oven at 60°C or freeze-dried from benzene. GPC of PVME solution in $CHCl_3$ gave $M_n = 74{,}000$ and $M_w/M_n = 1.83$. Films of PS/PVME blends were cast on glass slides from 5% toluene or chloroform solutions, evaporated for 1 day at ambient room conditions and dried *in vacuo* at 60°C for 3 days. Composition is specified by weight ratio. Thermal phase separation was accomplished by heating samples in a glass vessel to the specified temperature ±2°C for 30 min and followed by quenching at 0°C. The films were subsequently ground to a fine powder at −195°C in a Spex Freezer Mill (Spex Industries, Edison, NJ) in order to facilitate magic-angle spinning. NMR measurements were taken on an IBM 200 AF spectrometer equipped with an IBM Solids Accessory and Doty VT CP-MAS probe. Samples were generally spun at 4.5 kHz and cross-polarized for 2 ms at 50 kHz fields (5 μs 90° pulses for both ^{13}C and ^{1}H). Quadrature detection and phase alternation were used throughout. Semilog plots of data were analyzed for biphasic decay. $T_{1\rho}^{H}$ was measured through change in CP carbon intensity after variable ^{1}H spin lock time, τ, by the method of Schaeffer.[20] After the time τ, CP was held for 2 ms. Cloud point measurements were made with a laser scattering apparatus with total scattering detector.[11]

RESULTS

^{13}C-CP-MAS spectra of pure PVME and of a 60/40 PS/PVME blend at −5°C are shown in Figure 1. PVME which is a very viscous fluid at room

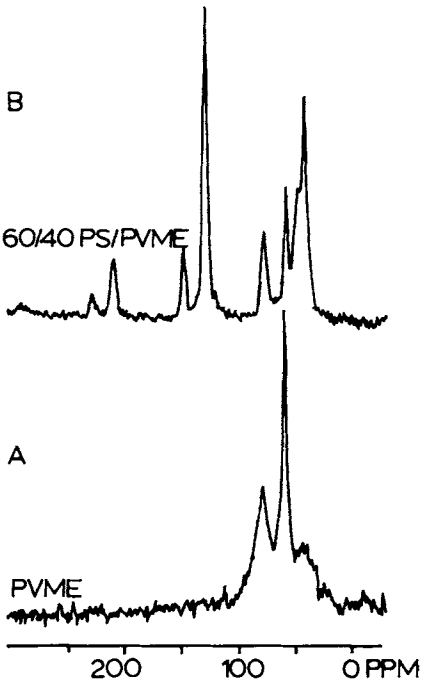

Fig. 1. Cross polarization spectra of (a) pure PVME (64 scans) and (b) a 60/40 PS/PVME blend (1000 scans). Both spectra were obtained at −5°C under identical conditions, thus demonstrating observability of even pure PVME by cross polarization under these conditions (2 ms spin lock time).

temperature cannot be cross-polarized effectively. However, at −5°C a strong signal is easily obtained by cross polarization. If one notes that the spectrum of the 60/40 blend was obtained with 1000 scans and the pure PVME spectrum with only 64, the observed relative signal to noise ratio of 4 between the two spectra is as expected if PVME is detected efficiently in both samples. The observed 59 ppm peak is very nearly 40% of the height of the peak in pure PVME. Thus at −5°C we are observing virtually all PVME present and would detect any pure PVME phase present in significant concentration. The proton spin–lattice relaxation time in the laboratory frame, T_1^H, was determined for 75/25 and 50/50 blends of PS/PVME prepared by freeze-drying of benzene solutions. The results are given in Table I together with T_1^H values for the homopolymers of the protons of the C_α (aromatic C_1), C_β (aromatic $C_{2\text{-}6}$), C_γ (OCH), C_δ (OCH_3), and C_ϵ (backbone carbons) sites.

The dependence of $T_{1\rho}^H$ on molecular weight was investigated for 75/25 and 50/50 blends. The data are shown in Table II. Molecular weight effects are detectable but small. In the 75/25 blends there is a modest but consistent increase of about 12% over the MW range of $T_{1\rho}^H$ with increasing PS molecular weight. For the 50/50 blend the only consistent difference is the 10–20% increase in $T_{1\rho}^H$ with PS MW > 9 K. The changes are greater than the approximate 7% nominal reproducibility.

The spin–lattice relaxation times for protons in the rotating frame, $T_{1\rho}^H$, were measured for PS (100 K)/PVME blends from 100 to 0% PS at 10 or 5%

TABLE I
Proton Spin-Lattice Relaxation Times for Blends and Homopolymers[a]

Proton/carbon site	T_1 (s) PS	75PS/25PVME	50PS/50PVME	PVME
H_α	1.83 ± 0.02	2.08 ± 0.03	2.30 ± 0.03	
H_β	1.93 ± 0.02	2.14 ± 0.008	2.12 ± 0.007	
H_γ		2.31 ± 0.04	1.91 ± 0.04	0.76 ± 0.01
H_δ		2.18 ± 0.05	2.11 ± 0.02	0.60 ± 0.03
H_ϵ	1.93 ± 0.02	2.11 ± 0.01	1.96 ± 0.01	
Av	1.90 ± 0.06	2.14 ± 0.09	2.08 ± 0.19	0.68 ± 0.08

[a] C_α (aromatic C_1), C_β (aromatic $C_{2\text{-}6}$), C_γ (OCH), C_δ (OCH_3), and C_ϵ (backbone carbons) sites.

intervals. All the ^{13}C resonances for the blends decay exponentially at 23°C as illustrated in Figure 2. The $T_{1\rho}^H$ values observed at 23°C by the ^{13}C-NMR are summarized in Table III. The data show a definite sensitivity of $T_{1\rho}^H$ to overall blend composition over the entire range of composition. The $T_{1\rho}^H$ at the aromatic carbon sites decrease monotonically with increasing PVME in the blend. The relaxation times of PVME and PS are practically equal from 90/10 to 60/40 composition within experimental accuracy. Two separate preparations of 70/30 blends have the same relaxation behavior. For blends rich in PVME, the C_γ and C_δ sites have shorter $T_{1\rho}^H$ than the others.

In order to optimize the observability of the PVME peaks for $T_{1\rho}^H$ measurements, a variable temperature study was done, the results of which are shown in Figure 3. This graph shows that both for the three blends and for the PVME homopolymer $\langle T_{1\rho}^H \rangle$ (see caption of Figure 3 for definition of average $T_{1\rho}^H$) approaches a minimum near room temperature. Here the averaging is done for $T_{1\rho}^H$ measured at each resolved peak of each species in the ^{13}C spectrum. The detectability via CP pulse sequences becomes very limited near and above room temperature. Nevertheless, it is clear that at −5°C there is maximal difference between $T_{1\rho}^H$ for the homopolymers; at that temperature pure PVME homopolymer is easily observable. This point was also made in discussing Figure 1.

The values of $T_{1\rho}^H$ at −5°C for protons at each carbon in a range of blends

TABLE II
Variation of $T_{1\rho}^H$ at 25°C with PS Molecular Weight

PS MW	$T_{1\rho}^H$ (ms) 75PS/25PVME 9 K	100 K	900 K	50PS/50PVME 9 K	100 K	900 K
H_α	3.90	3.86	3.90	1.77	2.16	2.08
H_β	3.87	4.06	4.3	1.74	2.32	2.1
H_γ	3.34	3.45	4.0	1.1		
H_δ		3.62	3.90	1.13	1.30	1.41
H_ϵ	3.79	3.87	4.4	1.71	2.20	2.08

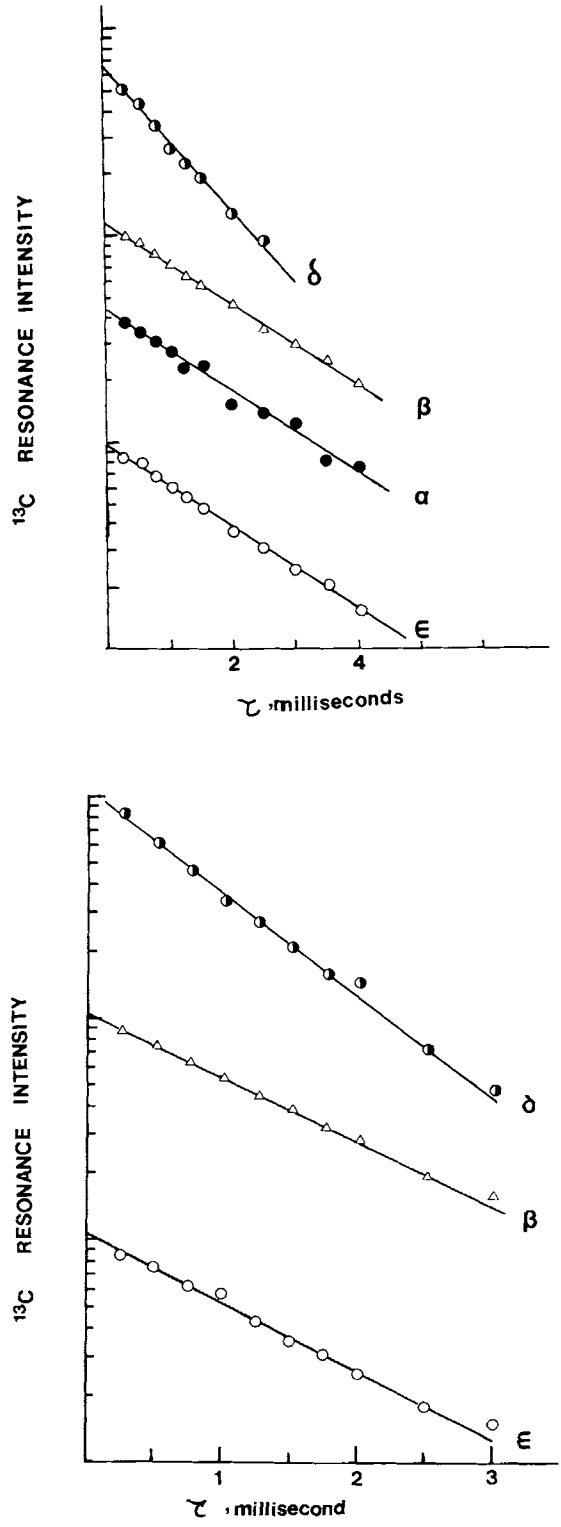

Fig. 2. Decay of ^{13}C intensity as a function of proton spin lock time at 23°C: (a) PS 40/PVME 60 blend; (b) PS 30/PVME 70 blend. For clarity each line is begun at a separate origin on the y-axis.

TABLE III
Rotating Frame $T_{1\rho}^{H}$ Relaxation Times at 23°C

Proton/carbon site	$T_{1\rho}^{H}$ (ms) for blend composition, PS% (100 K)												
	100	90	80	75	70	60	50	40	30	25	20	10	0
H_α	5.95	5.65	4.84	3.86	3.63[a] 3.60	3.16	2.16	2.24	b	1.85	b		
H_β	5.76	5.23	4.62	4.06	4.07 3.95	3.17	2.32	2.24	1.51	1.31	1.44	1.80	
H_γ		b	4.74	3.45	4.93 3.30	3.60	b	b	b	1.14	b	1.05	0.30
H_δ		b	4.88	3.62	4.01 3.88	b	1.28	1.30	0.95	0.78	0.97	b	0.77
H_ϵ	5.13	5.46	4.81	3.87	3.98 4.34	3.20	2.24	2.20	1.44	b	1.23	1.80	

[a] Duplicate blend preparations.
[b] Peaks too weak for precise relaxation time measurement.

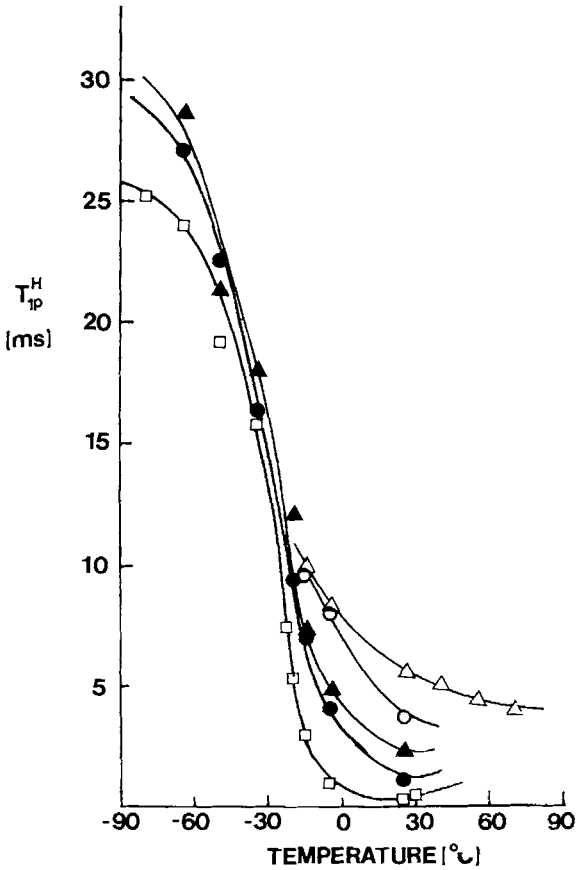

Fig. 3. Variation of $\langle T_{1\rho}^{H} \rangle$ with temperature for: (△) PS; (○) PS 75/PVME 25 blend; (▲) PS 50/PVME 50 blend; (●) PS 25/PVME 75 blend; (□) PVME. $\langle T_{1\rho}^{H} \rangle$ is the average of relaxation times of H_α, H_β, H_γ, H_δ, and H_ϵ.

were determined and are given in Table IV. For blends very rich in PS (> 80%) the C_γ and C_δ resonances of PVME were too weak to be observed. The latter became observable in blends containing PS < 75%. The data is similar to the room temperature results in some respects. For instance, $T_{1\rho}^H$ values for all the carbon sites are uniform for blends having 90–60% PS and the PVME protons have shorter relaxation times than the PS protons for blends with more than 40% PVME. However, there are also important differences. At −5°C the relaxation time is insensitive to blend composition between 60% < PS < 90%; the decay of spin magnetization is biphasic for blends with PS < 40% as illustrated in Figure 4 for 40 and 20% PS blends.

Thermal treatment of PS (100 K)/PVME blends at temperatures between 25 and 130°C did not result in phase separation as indicated by single exponential relaxation. Heating to > 140°C resulted in phase separation; the two phases have different $T_{1\rho}^H$ values (Table V). The relaxation times of the PS and PVME protons in the phase separated blends are not the same as their values in the homopolymers, thus indicating that each of the separated phases is a blend of compositions differing from the overall composition and that there is no separate domain of one or the other homopolymer. The observations are quite similar to the earlier reports on blend studies of limited compositions.[13-15,18]

In order to study the molecular weight effect on phase separation some PS (900 K)/PVME blends were also thermally treated over a range of temperatures from 120 to 159°C, yielding the $T_{1\rho}^H$ data of Table VI. Clearly the data are sensitive to blend compositions and annealing temperature. It is also evident that the ^{13}C decay is not single exponential and two $T_{1\rho}^H$ values are extracted from the decay of magnetization.

TABLE IV
Rotating Frame Relaxation Times at −5°C

Proton/carbon site	$T_{1\rho}^H$ (ms) for blend composition, PS% (100 K)											
	100	90	80	75	70	60	50	40	30	25	20	0
H_α	8.03	6.84	a	8.22	8.47[b] 8.30	a	a	6.29	5.17	4.25	a	
H_β	8.52	7.06	8.36	8.07	8.33 7.70	7.57	5.23	5.67	4.54	4.55	3.77	
H_γ	a	a	a	7.04	9.60 9.18	7.81	4.53	(0.90)[c] 6.02	(0.65) 3.30	(0.5) 3.39	(0.51)[c] 3.12	0.94
H_δ	a	a	a	a	8.60 8.44	7.0	4.17	(0.74)[c] 5.12	(0.70) 3.40	(0.5) 4.53	(0.66)[c] 2.82	1.03
H_r	8.58	7.50	8.16	8.51	7.66	7.50 7.40	4.23	(0.74) 6.07	(0.61) 3.91	(0.60) 3.27	(0.64) 3.53	

[a] Peaks are too weak for accurate relaxation time determination.
[b] Duplicate blend preparations.
[c] Value in parenthesis is initial decay for biphasic relaxation.

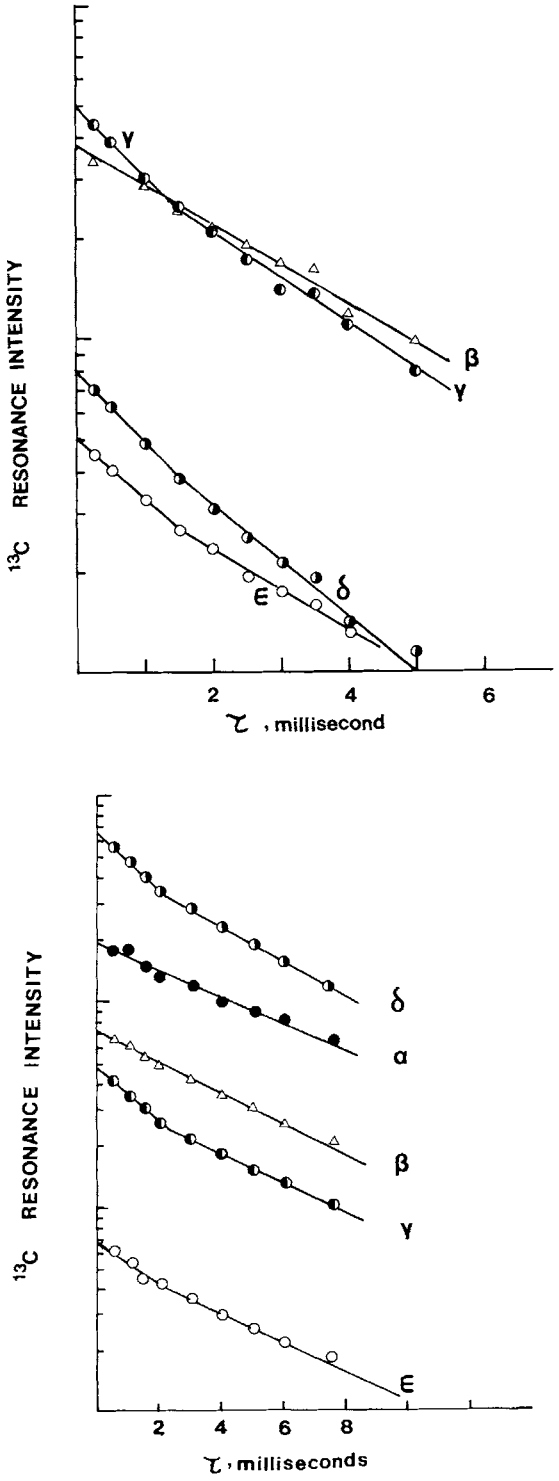

Fig. 4. Decay of ^{13}C intensity at −5°C, (a) PS 20/PVME 80 blend and (b) PS 40/PVME 60 blend as a function of spin lock time.

TABLE V
$T_{1\rho}^{H}$ of Phase-Separated PS (100 K) PVME Blends

PS/PVME initial blend	Temp of heat treatment[a] (°C)	$T_{1\rho}^{H}$ (ms) Short	Long
50/50	184	1.02	4.64
50/50	170	1.18	5.60
75/25	150	1.23	4.96
75/25	140	1.44	4.67
75/25	130	3.84[b]	

[a] Heating for 30 min.
[b] Single exponential decay.

DISCUSSION OF RESULTS

Though many experimental techniques have been used to measure miscibility of polymer blends, NMR is a powerful addition capable of measuring blend homogeneity at the molecular level. A blend is homogeneous on a segmental scale if the constituent polymers average to the same relaxation time. This averaging process is possible through spin diffusion and has been demonstrated for a number of blends.[2] Relaxation measurements were made in the laboratory frame for each component with T_1^H of the order of seconds. A common T_1^H indicates homogeneity in the coherence scale of tens of nanometers. Measurements in the rotating frame have $T_{1\rho}^H$ of the order of milliseconds, and a common $T_{1\rho}^H$ implies segmental uniformity on a scale of a few nanometers.

PS/PVME is one of the best known and most widely studied examples of a compatible blend system. The T_1^H values in the laboratory frame are the same for all the protons in the blends of any composition as confirmed in Table I. The molecular contacts are uniform over a coherence scale L given by[2]

$$\langle L^2 \rangle \simeq (T_1/T_2)\langle l_0^2 \rangle \tag{1}$$

TABLE VI
Relaxation Data for PS (900 K)/PVME Blends Treated at Higher Temperatures

$T_{1\rho}^{H}$ (ms)	50/50			75/25		30/70	
	139°C	149°C	159°C	149°C	159°C	130°C	116°C
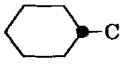	3.6 (0.85)	3.5 (1.26)	5.4 (1.02)	4.6 (1.2)	5.0 (2.0)		
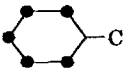	3.7 (0.99)	4.0 (0.95)	4.8 (1.10)	4.6 (1.1)	5.3 (1.53)	2.2 (0.53)	1.6 (0.52)
$CHCH_2$ (40 ppm)	3.4 (0.87)	3.5 (1.22)	4.5 (1.46)	4.4 (1.26)	5.8 (1.63)	2.0	1.6

where T_1 and T_2 are spin–lattice and spin–spin relaxation times and l_0 is the average distance between protons. For $T_2 = 10$ μs, $l_0 = 0.1$ nm and $T_1 = 1$ s, $L = 30$ nm. For $T_{1\rho} \simeq 1$ ms, $L \simeq 1$ nm, which is $(1000)^{1/2}$ times smaller.

A simple linear model has been developed[22] on the observed uniform relaxation rate of a given component containing a certain number of protons. Spin diffusion can average the relaxation of various types of protons in a homogeneous blend so that they have the same relaxation time

$$T_{1,AB}^{-1} = \frac{N_A M_A}{N_{Tot} T_{1A}} + \frac{N_B M_B}{N_{Tot} T_{1B}} \tag{2}$$

where A and B are components of blend A/B, M_i is the mole fraction of component i, N_i is the number of protons of component i, and $N_{Tot} = N_A M_A + N_B M_B$. In this model, the contribution to the relaxation time by a component has its relaxation time weighted by the number of its diffusing protons. According to eq. (2), the calculated T_1^H values for the 75/25 and 50/50 are 1.2 and 0.94 s, respectively, which are only about one-half of the observed relaxation times given in Table I. As only one T_1^H is observed, this indicates that the value of T_1^H for PVME in the blend is longer than T_1^H for the homopolymer. Thus blending PVME into PS strongly affects segmental dynamics of PVME.

The molecular weight effects evident in the data of Table II are small but somewhat surprising. As NMR relaxation times measure very local motions, they are not expected to depend on molecular weight after end group effects become negligible. No dependence of relaxation time on molecular weight is seen[23] for DP > 100. Yet it is also well known that phase separation is a strong function of molecular weight.[24] We have studied another compatible blend system, poly(phenylene oxide)/polystyrene[25] and have found pronounced molecular weight effects on microheterogeneity. Molecular weight effects on relaxation via entanglements have also been discussed[26] but these are probably not important below T_g.

The 25°C $T_{1\rho}^H$ data of Table III show an overall trend of decreasing $T_{1\rho}^H$ with increasing PVME content; the irregularities are probably due to temperature fluctuation. For each blend composition between 100 and 60% PS, the protons of PVME and of PS have a uniform $T_{1\rho}^H$ distinct to that composition. Only in blends having > 50% PVME are the relaxation times of PVME shorter than those protons on aromatic carbons of PS. All the decays of ^{13}C magnetization in Table II are simple exponential. Spins diffuse over a much smaller distance in the rotating frame experiments. The coherence scale is 10–20 Å for $T_{1\rho}^H$ of 1–5 ms. At this scale the blends rich in PS are homogeneous, but there is microheterogeneity in blends rich in PVME. However, at the much coarser scale of 300 Å all PS/PVME blends are homogeneous according to T_1^H as they are said to be compatible by other physical measurements.

The −5°C data of Table IV shows fairly uniform relaxation between 100 and 60% PS, which is insensitive to composition. The behavior changes with > 50% PVME: The PVME protons have shorter relaxation times than the aromatic protons and both types of protons relax faster with increasing PVME content. In addition, the ^{13}C magnetization decay is detectably biphasic when S/N is large as in the cases of 40 and 20% PVME blends, which suggests microphase separation of the 10-Å dimension at −5°C.

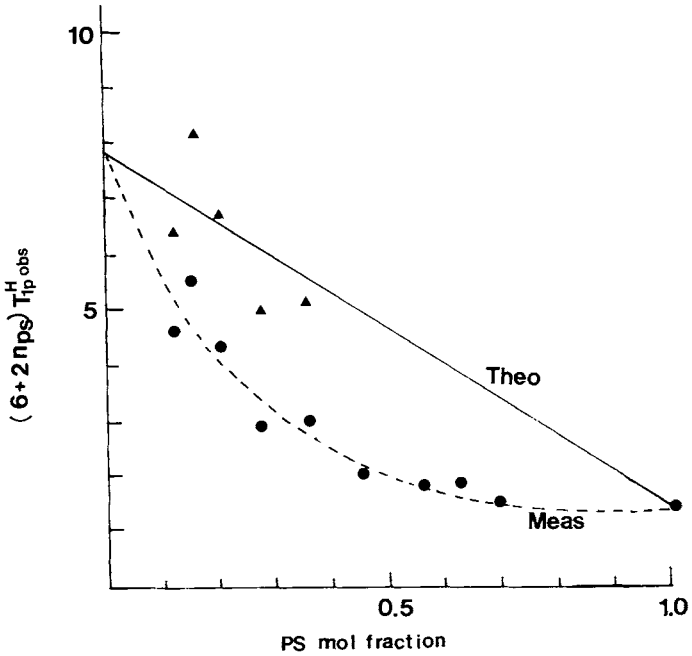

Fig. 5. Variation of $T^{H}_{1\rho}$ vs. PS content according to eq. (3): (- - -) experimental; (●) PS proton; (▲) PVME protons; (——) theoretical.

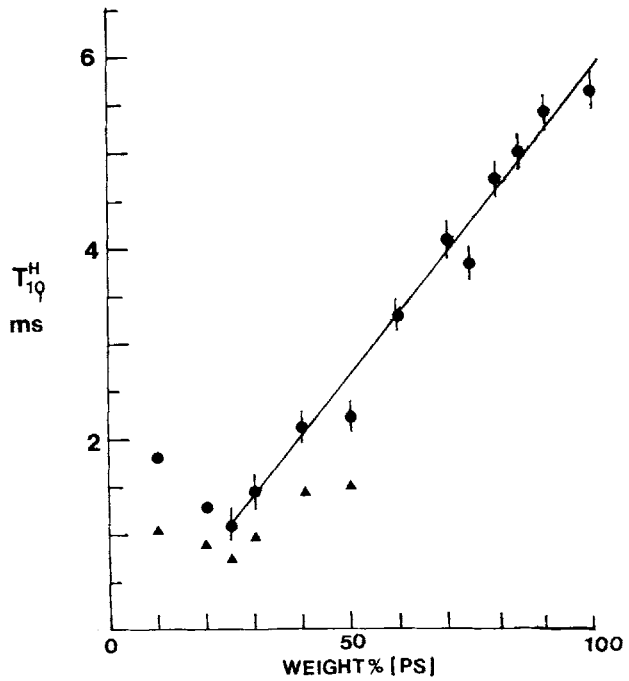

Fig. 6. Variation of $T^{H}_{1\rho}$ vs. wt % of PS. Symbols are the same as in Figure 5.

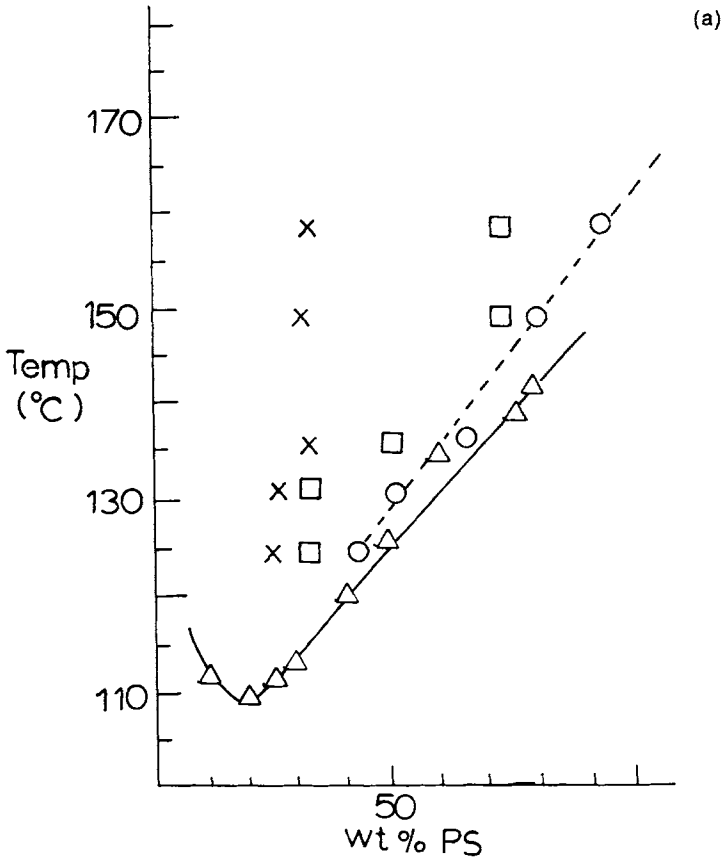

Fig. 7. LCST diagram for (a) PS (900 K)/PVME and (b) PS (100 K)/PVME blends: (△) cloud point; (□) initial, overall composition; (○) high PS phase composition determined by NMR, $T_{1\rho}^{H}$; (x) low PS phase composition rendered inaccurate by calibration problems explained in text.

The above data indicate two types of segmental scale regions of different composition, neither region being homopolymer. None of the $T_{1\rho}^{H}$ components corresponds to that of either homopolymer. Caravatti et al.[16] have interpreted their selective proton spin diffusion data to imply the coexistence of pure and mixed domains. Our low temperature data do not support this conclusion; however, their blends were prepared by solvent precipitation which may produce less homogeneous blends.

Applying the same linear additivity assumptions to $T_{1\rho}$, eq. (2) can be rewritten as

$$(6 + 2n_{PS})\frac{1}{T_{1\rho,Ob}^{H}} = \left(\frac{8}{T_{1\rho,PS}^{H}} - \frac{6}{T_{1\rho,PVME}^{H}}\right)n_{PS} + \frac{6}{T_{1\rho,PVME}^{H}} \qquad (3)$$

where $T_{1\rho,PS}^{H}$, $T_{1\rho,PVME}^{H}$, $T_{1\rho,Ob}^{H}$ are respectively the relaxation times of neat polystyrene, neat poly(vinyl methyl ether), and observed values for the blend containing n_{PS} mole fraction of styrene monomer. The data of Table III weighted according to eq. (3) are plotted in Figure 5, the straight line is that expected

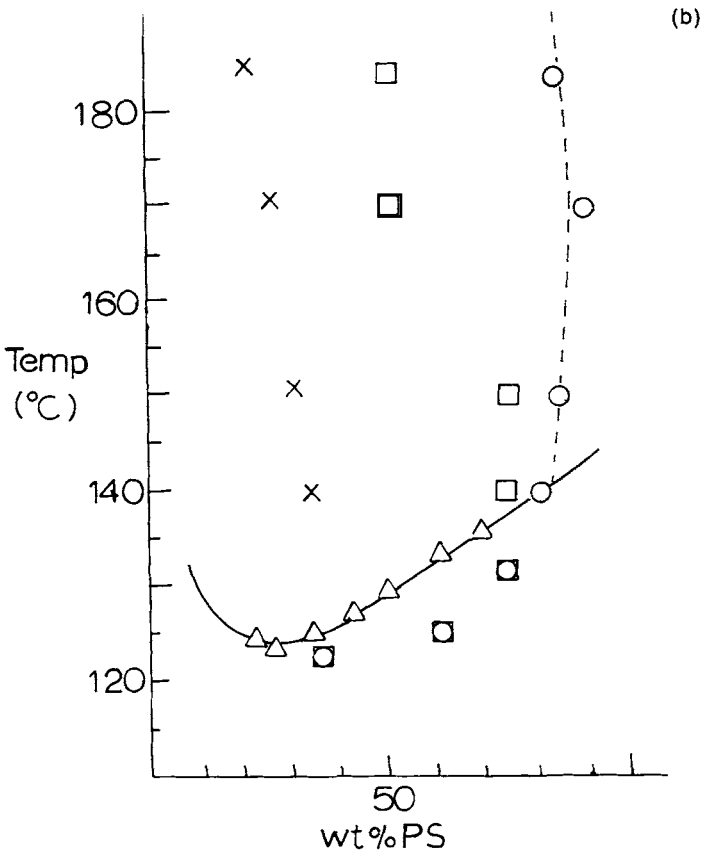

Fig. 7. (*Continued from the previous page.*)

for eq. (3). Clearly, the observed $T_{1\rho}^{H}$ do not follow the linear model so that these blends cannot be regarded as uniform on a segmental level.

In order to obtain the LCST phase diagram, one needs to calculate the phase compositions from the relaxation times. Figure 6 is a plot of $T_{1\rho}^{H}$ versus wt % of PS (100 K); the data are linear for PS content > 25%. This plot is useful as an empirical calibration curve. The observation that one set of the biphasic $T_{1\rho}^{H}$ data is linear down to $n_{PS} = 0.25$ suggests that the second $T_{1\rho}^{H}$ component for this composition range may be a minor species.

Figures 7(A) and 7(B) are phase diagrams constructed from the biphasic $T_{1\rho}^{H}$ data for thermally phase separated PVME blends with 900 and 100 K PS, respectively. Samples of the overall composition given by the abscissa of one of the dotted squares were heated to the temperature given by the ordinate. After 0.5 h, the sample was quenched in ice water and the NMR $T_{1\rho}^{H}$ experiment run at 23°C. The two $T_{1\rho}^{H}$ values were converted to component compositions by means of the linear part of Figure 5. Also included in Figure 7 is the cloud point curve which we have determined on the same samples. For the PS (900 K)/PVME blends the agreement of the cloud point and NMR determined curves for wt % PS > 30% is quite satisfactory. As expected from the deviations

in the calibration curve for lower PS concentrations, conversion of $T_{1\rho}^{H}$ to concentration in that region is unreliable. As cloud point determination of phase diagrams is measured by heating a given blend to the point of turbidity, and this NMR method is a measure of the final concentrations of the separated phases, the two methods need not necessarily give the same curve. The observations in Figure 7(A) that the cloud point curve falls below the NMR curve implies a small difference between the methods, although this difference is just beyond the size of experimental error for the NMR method. This difference would mean that cloud point detects concentration fluctuations which occur (as the temperature is increased) at concentrations lower than the final phase separated concentration. This small discrepancy could also reflect the 30-min heating time for the NMR samples which may be insufficient for completion of the slow stage of phase separation. Some preliminary NMR data showed small changes after 2 h, but autoxidation may become a problem.

The NMR-determined phase diagram for the PS (100 K)/PVME blend shows less agreement with the cloud point curve, although the region of the cloud point covers only a narrow temperature range which does not overlap the NMR data. Our thermal bath setup and the errors in NMR concentrations do not allow us to accurately follow such large composition changes over a narrow temperature interval as in seen in the PS (100 K)/PVME cloud point diagram.

The simple linear model of eqs. (2) and (3) fail for both T_1^H and $T_{1\rho}^{H}$. In the latter case, where data is extensive (Fig. 5), $T_{1\rho}^{H}$ of the blend is very close to that of homopolymer of styrene at PS > 60%. It was thought possible that the methyl protons of PVME may not be participating in the spin diffusion process by virtue of rapid rotation of the methyl group. However, elimination of these protons in eq. (3) resulted in a plot much like Figure 5. In this region of PS > 60% the $T_{1\rho}^{H}$ of PVME protons are nearly the same as the PS protons. It is as if the motion of PVME is constrained by PS but not vice versa. Yet, the T_g of PS/PVME blends decrease by 100°C when the composition changes from 100% PS to 60% PS.[5] The inherent difficulty with the simple linear model may be that the relaxation time is measured far below the T_g of PS and far above the T_g of PVME. Equation (2) was found to be valid for glass poly(4-methyl styrene)–poly(2,6-dimethylphenylene oxide) blends, in which case the T_g's of both component polymers are all much higher than the temperature of measurement.[22]

In conclusion, the PS/PVME blends have been said to be compatible according to macroscopic measurements of the ensemble system such as differential scanning calorimetry and dielectric relaxation.[5] These measurements indicate some molecular mixing occurs, but that the mixing is not as intimate as in random copolymers. The present NMR results indicate homogeneous mixing at 100-Å scale, but there is microheterogeneity at 10-Å scale, especially at high PVME contents and low temperatures. This microheterogeneity must be related to some form of segmental clusters possibly related to statistical composition fluctuations. We have demonstrated that solid NMR can be used to estimate LCST phase diagram.

The work was supported in part by the Materials Research Laboratories of the National Science Foundation at the University of Massachusetts.

References

1. D. Patterson and G. Delmas, *Trans. Faraday Soc.*, **65,** 708 (1969).
2. B. E. Eichinger and P. J. Flory, *Trans. Faraday Soc.*, **64,** 2035 (1968).
3. L. P. McMaster, *Macromolecules,* **6,** 760 (1973).
4. M. Bank, J. Leffingwell, and C. Thies, *Macromolecules,* **4,** 43 (1971).
5. M. Bank, J. Leffingwell, and C. Thies, *J. Polym. Sci. Polym. Phys. Ed.,* **10,** 1097 (1972).
6. R. Gelles and C. W. Frank, *Macromolecules,* **15,** 1486 (1982).
7. J. W. Cahn and J. E. Hilliard, *J. Chem. Phys.:* (a) **29,** 258 (1958); (b) **31,** 688 (1959).
8. H. L. Snyder, P. Meakin, and S. Reisch, *Macromolecules,* **16,** 757 (1983).
9. T. Hashimoto, J. Kumaki, and H. Kawai, *Macromolecules,* **16,** 641 (1983).
10. M. Shibayama, H. Yang, R. S. Stein, and C. C. Han, *Macromolecules,* **18,** 2179 (1985).
11. H. Yang, M. Shibayama, R. S. Stein, N. Shimuzu, and T. Hashimoto, *Macromolecules,* **19,** 1667 (1986).
12. F. J. Lu, E. Benedetti, and S. L. Hsu, *Macromolecules,* **16,** 1525 (1983).
13. T. K. Kwei, T. Nishi, and R. F. Roberts, *Macromolecules,* **7,** 667 (1974).
14. T. Nishi, T. T. Wang, and T. K. Kwei, *Macromolecules,* **8,** 227 (1975).
15. T. K. Kwei and T. T. Wang, in *Polymer Blends,* D. R. Paul and S. Newman, Eds., Academic, New York, 1978, Vol. I, pp. 141–184.
16. P. Caravatti, P. Neuenschwander, and R. R. Ernst, *Macromolecules:* (a) **18,** 119 (1985); (b) **19,** 1889 (1986).
17. E. O. Stejskal, J. Schaefer, M. D. Sefeik, and R. A. McKay, *Macromolecules,* **14,** 275 (1981).
18. S. Kaplan, *Am. Chem. Soc. Polym. Prepr.* **25,** 356 (1984).
19. G. C. Gobbi, R. Silvestri, T. P. Russell, J. R. Lyerla, W. Fleming, and T. Nishi, *J. Polym. Sci. Polym. Lett. Ed.,* **25,** 61 (1987).
20. J. Schaefer, E. O. Stejskal, and R. Buchdahl, *Macromolecules* **10,** 384 (1977).
21. V. J. McBrierty and D. C. Douglas, *J. Polym. Sci. Macromol. Rev.,* **16,** 295 (1981).
22. L. C. Dickinson, H. Yang, C.-W. Chu, R. S. Stein, and J. C. W. Chien, *Macromolecules,* **20,** 1757 (1987).
23. A. Allerhand and R. K. Mailstone, *J. Chem. Phys.* **56,** 3718 (1972).
24. D. R. Paul and S. Newman, *Polymer Blends,* Academic, New York, 1978.
25. S. Li, L. C. Dickinson, J. C. W. Chien, S. Lin, *Macromolecules,* to appear.
26. R. A. Komoroski and L. Mandelkern, in *Applications of Polymer Spectroscopy,* E. G. Brame, Ed., Academic, New York, 1978.

Received August 23, 1989
Accepted February 16, 1990